Mutagenesis, 2016, 31, 481–490
doi:10.1093/mutage/gew014
Original Manuscript
Advance Access publication 31 March 2016

OXFORD

Original Manuscript

Cell cycle dependent cellular uptake of zinc oxide nanoparticles in human epidermal cells

Pal Patel[1], Krupa Kansara[1], Violet Aileen Senapati[1], Rishi Shanker[1], Alok Dhawan[1,2] and Ashutosh Kumar[1,*]

[1]Institute of Life Sciences, School of Science and Technology, Ahmedabad University, University Road, Ahmedabad 380009, Gujarat, India and [2]CSIR-Indian Institute of Toxicology Research, Mahatma Gandhi Marg, PO Box 80, Lucknow 226001, Uttar Pradesh, India

*To whom correspondence should be addressed. Tel: +91 79 26302414; Fax: +91 79 26302419; Email: ashutosh.kumar@ahduni.edu.in

ILS communication Number: 55.

Received 13 October 2015; Revised 2 February 2016; Accepted 1 March 2016.

Abstract

Metal oxide nanoparticles (NPs), including zinc oxide (ZnO) NPs have shown success for use as vehicles for drug delivery and targeting gene delivery in many diseases like cancer. Current anticancer chemotherapeutics fail to effectively differentiate between cancerous and normal cells. There is an urgent need to develop novel drug delivery system that can better target cancer cells while sparing normal cells and tissues. Particularly, ZnO NPs exhibit a high degree of cancer cell selectivity and induce cell death, oxidative stress, interference with the cell cycle progression and genotoxicity in cancerous cells. In this scenario, effective cellular uptake of NP seems to be crucial, which is shown to be affected by cell cycle progression. In the present study, the cytotoxic potential of ZnO NPs and the effect of different cell cycle phases on the uptake of ZnO NPs were examined in A431 cells. It is shown that the ZnO NPs led to cell death and reactive oxygen species generation and were able to induce cell cycle arrest in S and G_2/M phase with the higher uptake in G_2/M phase compared with other phases.

Nanoparticles (NPs) are considered as a promising candidate in targeted therapies due to their improved bioavailability and specificity for application in several diseases including cancer (1,2). Therapeutic agent or drugs can be encapsulated within NPs or can be absorbed or conjugated onto their surface (3). Applications of NPs as vehicles for drug delivery are currently an area of intense research. Current anticancer chemotherapeutics fail to produce a complete anticancer response due to the development of drug resistance or the failure to effectively differentiate between cancerous and normal cells (4). Hence, it is imperative to develop a novel drug delivery system that can efficiently target the cancer cells while sparing normal cells and tissues.

A variety of metal oxide NPs have a good potential for their use as vehicle for drug delivery, targeted gene delivery and tumour imaging (5). Use of zinc oxide (ZnO) NPs provides considerable promise in this domain, as ZnO NPs exhibit a high degree of cancer cell selectivity (5–8). ZnO NPs have multiple properties including favourable band gap, electrostatic charge, surface chemistry and potentiation of redox-cycling cascades that are useful for biomedical applications (5). ZnO NPs have also found applications in areas of drug carrier and targeted gene delivery (9,10).

Earlier studies have shown that ZnO NPs induce cell death, oxidative stress, interfere with the cell cycle progression and genotoxicity in different organ-specific mammalian cell lines and in mice indicating their (11–15) inherent anticancer cytotoxic potential (5). NPs can easily enter into the cell and interact with cellular system using energy dependent pathways (16). Due to this behaviour, NPs interactions with biological systems were investigated for their potential to target tumour (17).

Physico-chemical properties of NPs including size, shape, surface charge and surface chemistry play an important role in their cellular uptake (18–20). The uptake of NPs in cells is also influenced by the different cell cycle phases (20). The protein corona also plays an important role in the internalisation of NPs in the cells. Additionally, the interaction of NPs with cellular proteins is also dependent on cell cycle phases, as the expression of membrane proteins can vary

© The Author 2016. Published by Oxford University Press on behalf of the UK Environmental Mutagen Society. All rights reserved.
For permissions, please e-mail: journals.permissions@oup.com.

Downloaded from https://academic.oup.com/mutage/article/31/4/481/1751667 by Ahmedabad University user on 01 May 2025

during the cell cycle phases (21). Earlier study from Kim *et al.* (20) have shown the effect of cell cycle phases on the cellular uptake of NPs using human lung carcinoma cells (A549) and carboxyl functionalised fluorescent tagged polystyrene NPs (PS-COOH) after 72 h. The uptake of NPs in the cells was observed maximum in G_2/M and subsequently in S and G_0/G_1 phase. It can be hypothesised from their observation that in cell cycle dependent targeted therapy, G_2/M phase is more favourable to improve NP uptake.

In the present study, we investigated the effect of different cell cycle phases on the uptake of ZnO NPs. Instead of considering uptake in non-synchronised population, the cells were arrested in individual phases of cell cycle and ZnO NPs uptake was evaluated. Our data suggest that the ZnO NPs have higher uptake in G_2/M and induce cell cycle arrest by activating the reactive oxygen species (ROS).

Materials and methods

Chemicals

Zinc oxide nanopowder (Cas No. PL-ZnO14-5g) was purchased from Reinste, Delhi, India. Phosphate buffered saline (PBS; Ca^{2+}, Mg^{2+} free), Dulbecco's Modified Eagles Medium (DMEM), antibiotic-antimycotic solution (10 000 U/ml penicillin, 10 mg/ml streptomycin and amphotericin-B), foetal bovine serum (FBS), Trypsin-EDTA, 2,5-diphenyltetrazolium bromide (MTT), neutral red (NR) dye, 2-7-dichlorofluorescein diacetate (DCF-DA) dye, propidium iodide (PI), Triton X-100, RNase, dimethyl sulphoxide (DMSO), thymidine were purchased from Hi-Media Pvt. Ltd, Mumbai, India. l-Mimosine and nocodazole were purchased from Sigma–Aldrich, St Louis, MO, USA. Tissue culture flasks (25 cm^2), 6-well plates and 96-well plates were purchased from Corning, India. Syringe filters (0.22 µm) and filter holders were purchased from Millipore Co. Pvt. Ltd, Mumbai, India. Syringe needles were purchased from Dispovan, India.

ZnO NPs preparation and characterisation

ZnO NPs were suspended in Milli-Q water and culture medium (DMEM + 10% FBS) at a concentration of 0.2 mg/ml, probe sonicated at 45 W for 10 min (2 min pulse on and 1 min pulse off). Hydrodynamic size and zeta potential of the stock suspension were determined by a Zeta Sizer Nano-ZS equipped with 4.0 mW, 633 nm laser (Model ZEN3600, Malvern, UK) instrument.

Cell culture and treatment of ZnO NPs

The human epidermal carcinoma cell line (A431) was obtained from National Centre for Cell Sciences, Pune, India, and cultured in DMEM supplemented with 10% FBS (heat inactivated), 0.2% sodium bicarbonate and 10 ml/L antibiotic and antimycotic solution, respectively at 37°C under a humidified atmosphere of 5% CO_2.

Stock suspension of ZnO NPs (200 µg/ml) in DMEM (supplemented with 10% FBS) was serially diluted to concentrations ranging from 1 to 200 µg/ml (corresponding to 0.31–62.5 µg/cm^2) for cytotoxicity assays (MTT and NR uptake), cellular uptake, ROS generation, cell cycle progression analysis, etc. For each experiment, the particle suspension was freshly prepared, diluted to appropriate concentrations and immediately applied to the cells. For different assays 96- and 6-well culture plates having a treatment volume of 0.1 and 2 ml, respectively were used. Culture medium without ZnO NPs was served as the control in each experiment.

Cytotoxicity assay

Cytotoxicity of A431 cells after exposure to ZnO NPs was determined by MTT [3-(4, 5-dimethylthiazoyl-2-yl) 2, 5-diphenyltetrazolium bromide] assay and NR uptake assays. MTT assay is based on the mitochondrial activity and was done according to the method of Mosmann (22). NR uptake assay is based on the accumulation of NR dye in the lysosomes of viable cells and was performed according to the method of Borenfreund and Puerner (23) with slight modification.

Briefly, 1×10^4 cells were seeded in 96-well plates and were maintained in culture media for 24 h. Cells were further exposed to different concentrations (1–200 µg/ml) of ZnO NPs for 6, 24 and 48 h. NP interference with the assay reagents was checked by incubating NPs with the assay reagents including dye and buffers using cell free system. The results were assessed by measuring the absorbance at their respective wavelengths using a SYNERGY-HT multiwell plate reader, Bio-Tek, USA using Gen5 software.

Intracellular ROS measurement

The level of intracellular ROS generation was estimated by the method of Wan *et al.* (24) further modified by Shukla *et al.* (25) using DCF-DA dye. Cells (3.0×10^5 cells/well) were seeded in a six-well plate and were exposed to different concentration of ZnO NPs (10–80 µg/ml) for 6 h. The ZnO NPs containing media was aspirated and the cells were washed twice with 1× PBS. Cells were harvested using 0.25% trypsin-EDTA and then centrifuged at 135*g* for 5 min. The supernatant was discarded and the pellet was resuspended in 1 ml of PBS containing DCF-DA (20 µM) and incubated for 30 min at 37°C. The level of intracellular ROS was measured both by flow cytometer (FACSCalibur, BD Bioscience, CA, USA) and fluorescent microscope (Model DM 2500 Leica, Wetzlar, Germany).

Cell cycle progression analysis

The distribution of DNA in the cell cycle was studied by flow cytometer. About 3×10^5 cells/well were seeded in six-well cell culture plates. Cells were exposed to different concentrations of ZnO NPs (10–80 µg/ml) for 6, 24 and 48 h. The treatment was removed and cells were harvested and centrifuged at 135*g* for 10 min at 37°C. The pellet was fixed in ice-cold ethanol (70% in 1× PBS) and incubated at –20°C for 30 min. Cells were centrifuged and resuspended in lysis buffer (0.2% triton in 1× PBS) and incubated at 4°C for 30 min. Cells were further centrifuged and resuspended in 20 µg/ml RNase prepared in 1× PBS, incubated at 37°C for 30 min. Further cells were centrifuged and resuspended in 1× PBS and stained with 10 µl PI (1 mg/ml) followed by incubation at 4°C until analysis by flow cytometry (FACSCalibur, BD Bioscience).

Cellular uptake of ZnO NPs

A431 cells were seeded in six-well plates at a density of 3×10^5 cells/well. After 24 h of incubation, ZnO NPs of different concentrations (10–80 µg/ml) were added into the wells and incubated for 6 h. After exposure, NPs were removed and cells were harvested using 0.25% trypsin-EDTA. The supernatant was discarded and the pellet was resuspended in 500 µl of 1× PBS and the uptake of particles was determined using flow cytometer (FACSCalibur, BD Bioscience).

Cell synchronisation in different cell cycle phases

G_0/G_1 phase (mimosine block)

About 1×10^5 cells per well were seeded in six-well cell culture plates and allowed to adhere for 24 h. Cells were then incubated with 500 µM mimosine prepared in DMEM (10% FBS) for 24 h. After incubation, cells were washed with 1× PBS and stained with PI and were analysed using flow cytometer (FACSCalibur, BD Bioscience).

Downloaded from https://academic.oup.com/mutage/article/31/4/481/1751667 by Ahmedabad University user on 01 May 2025

S phase (double thymidine block)

About 1×10^5 cells per well were seeded in six-well plate cell culture plates. Cells were incubated with 2 mM thymidine prepared in DMEM (10% FBS) for 19 h (First block). After first block, the thymidine was removed and DMEM + 10% FBS was added for 8 h to release cells. After releasing cells DMEM (10% FBS) + 2 mM thymidine were added for 18 h (second block). Finally, thymidine was removed by washing with 1× PBS. Cells were stained with PI and were analysed using flow cytometer (FACSCalibur, BD Bioscience).

G_2/M phase (nocodazole block)

About 1×10^5 cells per well were seeded in six-well cell culture plates. Cells were incubated with DMEM (10% FBS) + 50 ng/ml nocodazole for 15 h. After treatment, media were removed and cells were washed with 1× PBS. Cells were stained with PI and analysed using flow cytometer (FACSCalibur, BD Bioscience).

Cellular uptake of ZnO NPs in different cell phases after synchronisation

Cells were seeded and pre-treated with different cell synchronising chemicals as described above. After removing the synchronising chemicals, ZnO NPs (40, 60 and 80 µg/ml) were added into wells and incubated for different time intervals (6 and 24 h). After exposure, NPs were removed and cells were harvested, and samples were prepared according to the method described in Cellular uptake of ZnO NPs.

Statistical analysis

Results from each experiment were expressed as mean ± SEM (standard error of mean) of three individual experiments and data were analysed using one-way analysis of variance (ANOVA). In all cases, $P < 0.05$ was considered as significant.

Results

Characterisation of ZnO NPs

The average hydrodynamic size and zeta potential of ZnO NPs in Milli-Q water were 215.8 ± 0.1 nm and −25.3 ± 0.4 mV, respectively. However, in DMEM medium (with 10% FBS) the hydrodynamic size and the zeta potential were 30.9 ± 0.5 nm and −12.8 ± 0.6 mV, respectively (Figure 1).

Evaluation of ZnO NP induced cytotoxicity

Cell viability assays were performed to assess the short-term, non-cytotoxic concentration of ZnO NPs for A431 cells. Both MTT and NR uptake assays showing time and concentration dependent cytotoxicity of ZnO NPs in A431 cells.

MTT results demonstrated a statistically significant ($P < 0.05$) reduction in the mitochondrial succinate dehydrogenase enzymatic activity to 70.56% and 66.31% (relative to 100% of control) in cells exposed to ZnO NPs at concentration 100 and 200 µg/ml, respectively for 24 h. The reduction was further significant and reduced to 70.25%, 70.72%, 55.57% and 52.71% (relative to 100% of control) at 60, 80, 100 and 200 µg/ml concentrations, respectively after 48 h of exposure in human epidermal carcinoma (A431) cells. However, no significant cytotoxicity was observed in A431 cells after 6-h exposure (Figure 2A).

In the NR uptake assay, a statistically significant ($P < 0.05$) reduction in %NR uptake was observed at two higher concentrations (100 and 200 µg/ml) of ZnO NPs. NR uptake was reduced to 65.83% and 42.32% after 6 h and 44.25% and 31.39% after 24 h and 39.28% and 8.09% after 48 h, demonstrating a high cytotoxic effect of ZnO NPs in A431 cells (Figure 2B).

Intracellular ROS generation

Our data showed that ZnO NPs induced oxidative stress in A431 cells as evident from the increased intracellular ROS. A significant

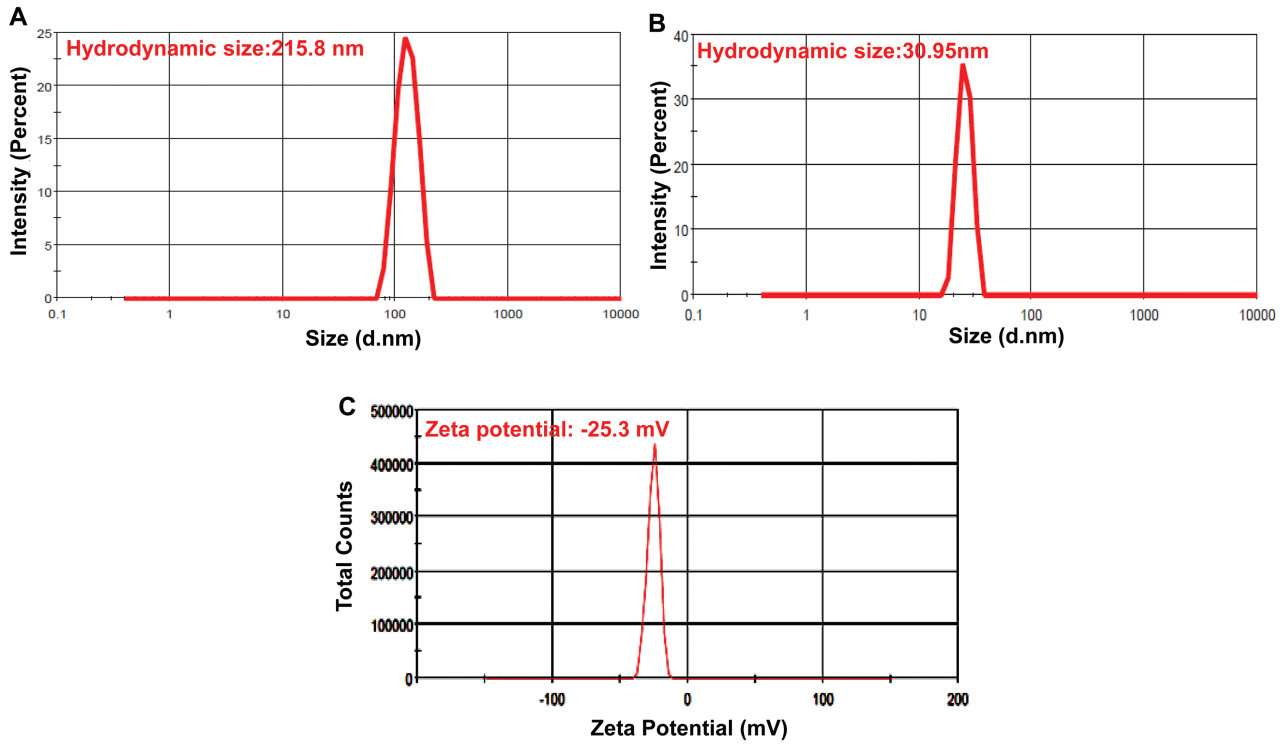


Figure 1. Characterisation of ZnO NPs by DLS. Hydrodynamic size of ZnO NPs in (**A**) Milli-Q water (**B**) DMEM + 10% FBS (**C**) Zeta potential of ZnO NPs in Milli-Q water.

Downloaded from https://academic.oup.com/mutage/article/31/4/481/1751667 by Ahmedabad University user on 01 May 2025

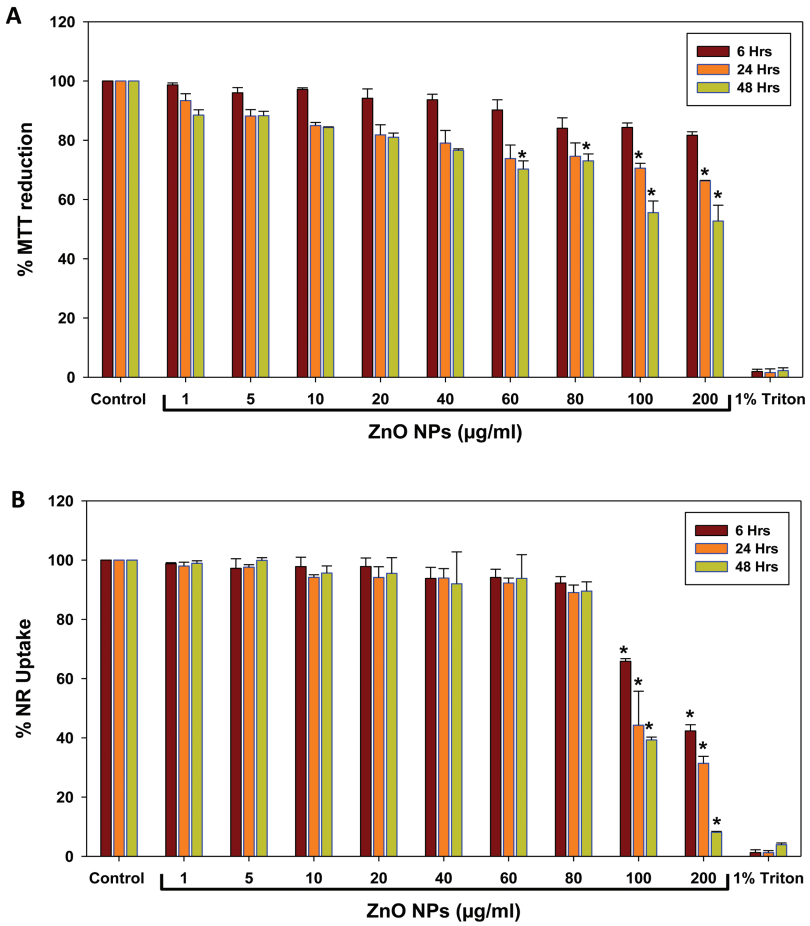


Figure 2. Cytotoxicity of ZnO NPs in human epidermal cells. (**A**) % MTT reduction (**B**) % NR uptake. Values are expressed as mean ± SEM for three independent experiments. *$P < 0.05$, compared with control.

($P < 0.05$) concentration dependent fold increase in ROS generation was observed in the form of increased fluorescence intensity on treatment with ZnO NPs (1.41, 2.54, 4.06 and 4.41 at 10, 20, 40 and 80 µg/ml, respectively; Figure 3B and C). The fluorescent microscope photographs also demonstrated and validated the data as observed in flow cytometry (Figure 3A).

Cell cycle analysis

ZnO NPs resulted in a decrease in number of cells in the G_1 phase and consequently a slight increase in number of cells in the S and G_2/M phases. In A431 cells, ZnO NPs have also been shown to induce cell cycle arrest in S and G_2/M phase in a concentration-dependent manner, however the data were not statistically significant (Figure 4).

Uptake of ZnO NPs

Using flow cytometry, we observed a statistically significant ($P < 0.05$) increase (151.48% and 257.03%) in the intensity of side scatter (SSC) of A431 cells after 6 h of ZnO NPs exposure to 40 and 80 µg/ml, relative to control cells (100%) (Figure 5).

Synchronisation of cells

To evaluate the role of cell cycle on the cellular uptake of ZnO NPs, synchronisation of cells in different phases (G_0/G_1, S and G_2/M) was done by different methods. Mimosine was used for G_0/G_1 phase synchronisation; thymidine was employed for S phase synchronisation and nocodazole treatment was for G_2/M phase cell synchronisation (Figure 6).

In control population, the percent of cells in G_0/G_1 phase was 50.65%. After mimosine treatment, the percent of cells that enter into G_0/G_1 phase increased to 81.55%. Before treatment with thymidine, 29.09% cells were found in S phase which increased to 80.56% after treatment. The percent of cells in G_2/M phase before and after treatment with nocodazole were found to be 31.37% and 90.21%, respectively.

Cellular uptake of ZnO NPs in different cell cycle phases

After the synchronisation of cells in different phases, the uptake of ZnO NPs was studied at different time intervals. Cells arrested in S and G_2/M phase showed higher uptake than cells arrested in G_0/G_1 phase after 6 h of ZnO NPs treatment. Difference in the uptake of ZnO NPs was also observed after 24 h of incubation. In G_0/G_1 phase uptake of NPs was less as compared to other phases. Cells which were present in S phase had higher intracellular NPs concentration than cells in G_0/G_1 phase and lower than the cells present in G_2/M phase. From the results, it is evident that maximum NPs uptake is observed in G_2/M phase followed by S phase and then in G_0/G_1 phase: $G_2/M > S > G_0/G_1$ (Figure 7; Table 1).

Discussion

In the present study, we investigated the cytotoxic potential and cell cycle dependent cellular uptake of ZnO NPs in A431 cells. Our data demonstrated that ZnO NPs are cytotoxic at high concentrations and generates oxidative stress due to increase in intracellular ROS,

Downloaded from https://academic.oup.com/mutage/article/31/4/481/1751667 by Ahmedabad University user on 01 May 2025

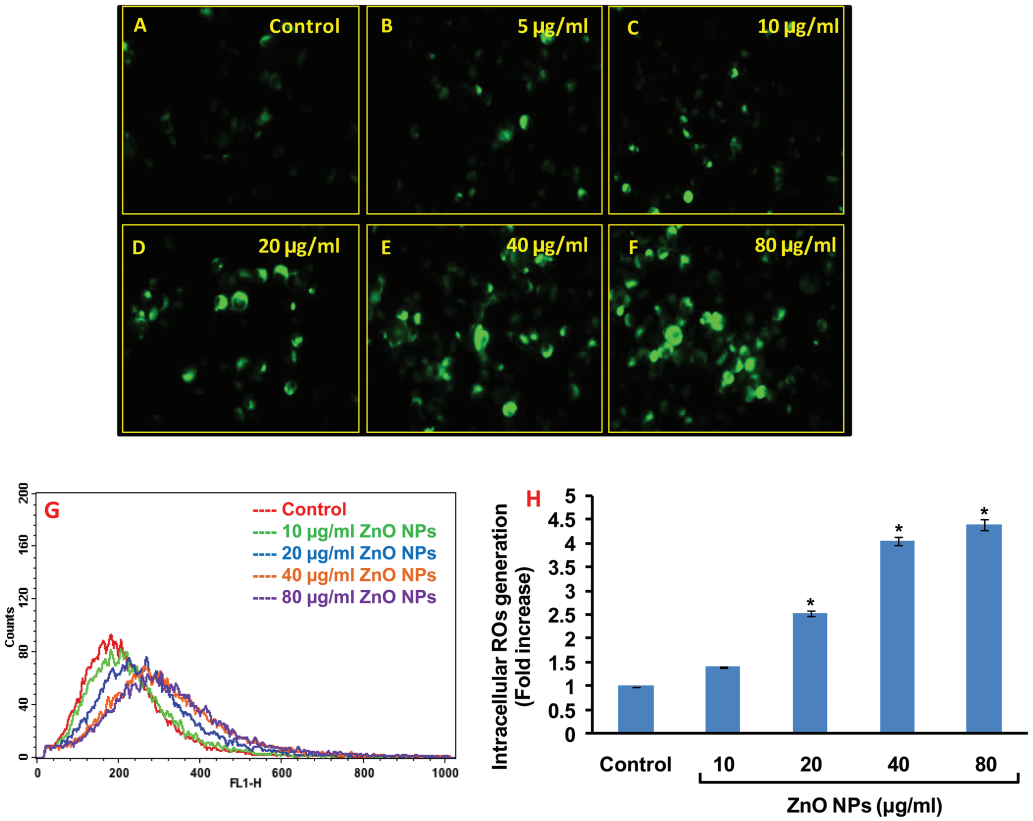


Figure 3. Intracellular ROS generation using DCFDA dye. Photomicrographs showing generation of ROS in A431 cells using DCFDA dye. (**A**) Control cells (**B–F**) cells treated with different concentration of ZnO NPs for 6 h. (Magnification ×400). (**G**) Histogram analysis of ROS generation by flow cytometer after ZnO NPs treatment to A431 cells for 6 h. (**H**) Bar graph representing a significant concentration dependent fold increase in intracellular ROS generation in A431 cells after treatment with ZnO NPs. Values represents mean ± SEM of three experiments. *$P < 0.05$, compared with control.

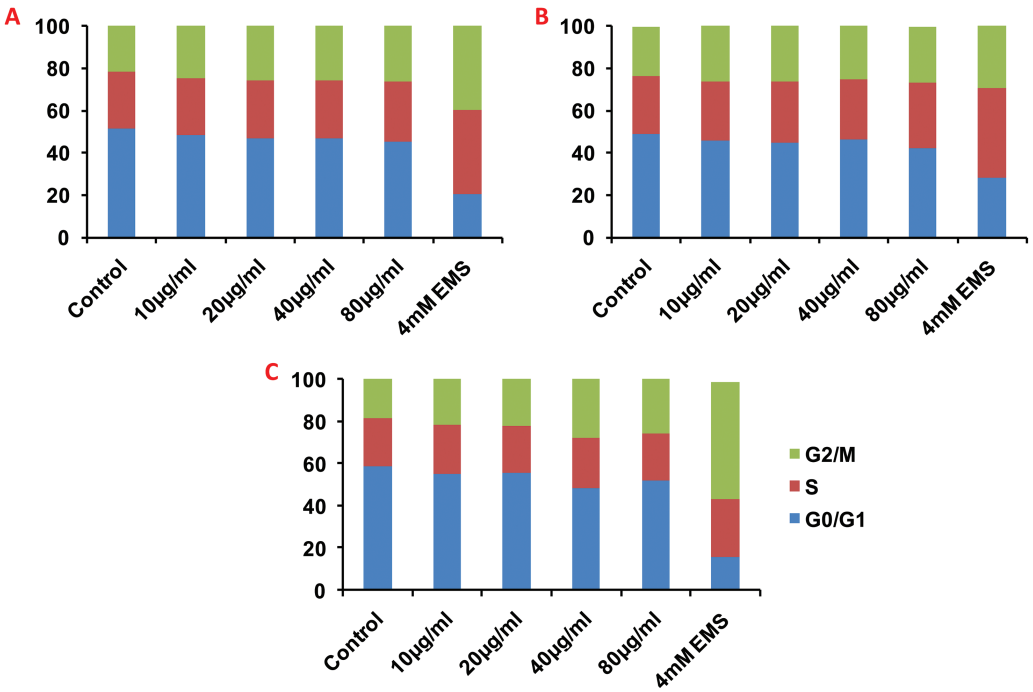


Figure 4. Cell cycle progression analysis of A431 cells after exposure of ZnO NPs. Bar graphs indicating the percent cell distribution in different phases of cell cycle (G_1, S and G_2/M) after treatment with ZnO NPs for (**A**) 6 h (**B**) 24 h and (**C**) 48 h.

Downloaded from https://academic.oup.com/mutage/article/31/4/481/1751667 by Ahmedabad University user on 01 May 2025

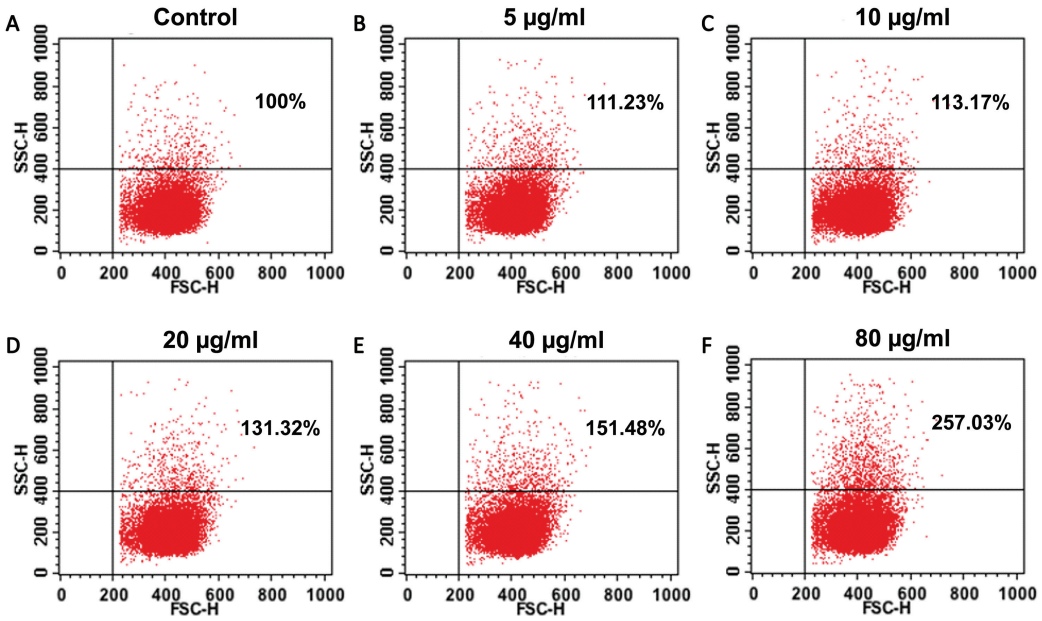


Figure 5. Cellular uptake of ZnO NPs in A431 cells after 6 h. Internalisation of ZnO NPs by flow cytometric parameter viz. SSC intensity. (**A**) Control cells. (**B–F**) Cells treated with ZnO NPs (5–80 µg/ml). Data represents mean ± SEM of three experiments. $*P < 0.05$, when compared with control.

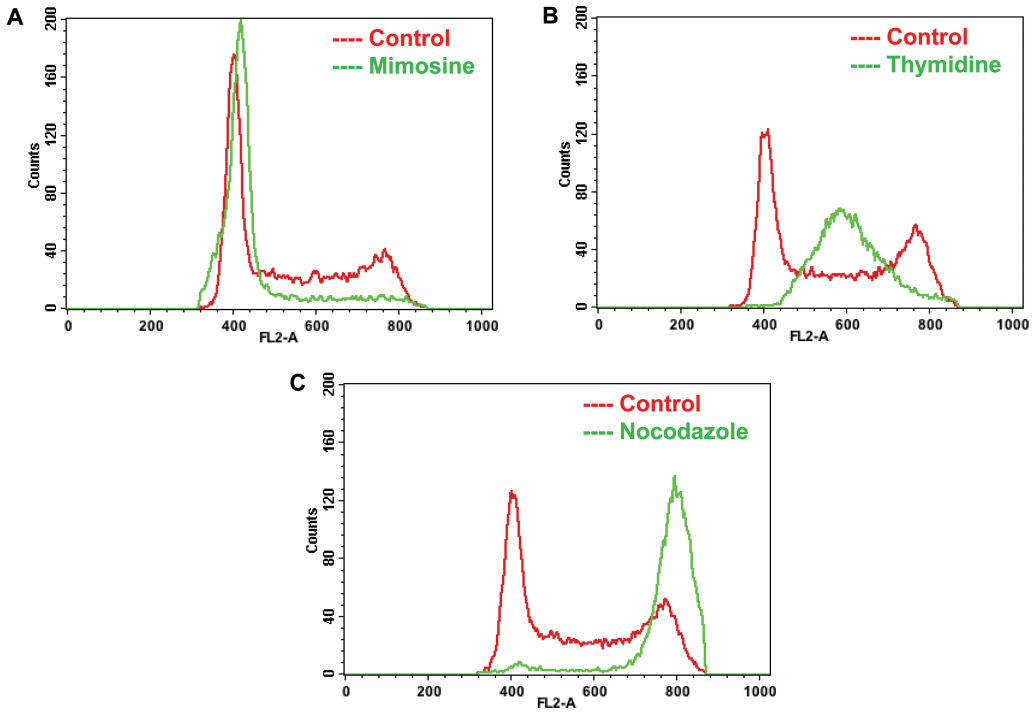


Figure 6. Cell cycle distribution before and after synchronisation. (**A**) Synchronisation in G_0/G_1 phase by mimosine. (**B**) Synchronisation in S phase by thymidine. (**C**) Synchronisation in G_2/M phase by nocodazole.

which could further lead to cell cycle arrest. We also observed cell cycle dependent cellular uptake of ZnO NPs in A431 cells.

Characterisation of NPs is the most essential part in nano-toxicological study. Dynamic light scattering (DLS) is considered as an indispensable tool for size characterisation as compared with other methods as it gives information for the stability of NPs in aqueous medium as well as the size is measured under conditions resembling the exposure scenarios. The size of ZnO NPs obtained in Milli-Q water and complete medium (DMEM + 10% FBS) were 215.8 and 30.9 nm, respectively. However, the size reported by its commercial supplier (Reinste) was 14 nm, as measured by transmission electron microscopy. The difference in the observed size of ZnO NPs is due to the different principles applied in the size measurement. Also, when NPs is exposed to biological medium, surface of NP gets coated with a layer of biomolecules especially proteins which forms 'protein corona'. In culture medium (DMEM + 10% FBS), ZnO NPs showed a small hydrodynamic size (30.9 nm) with a low zeta potential (−12.8 mV) because FBS forms a protein corona around the NPs

Downloaded from https://academic.oup.com/mutage/article/31/4/481/1751667 by Ahmedabad University user on 01 May 2025

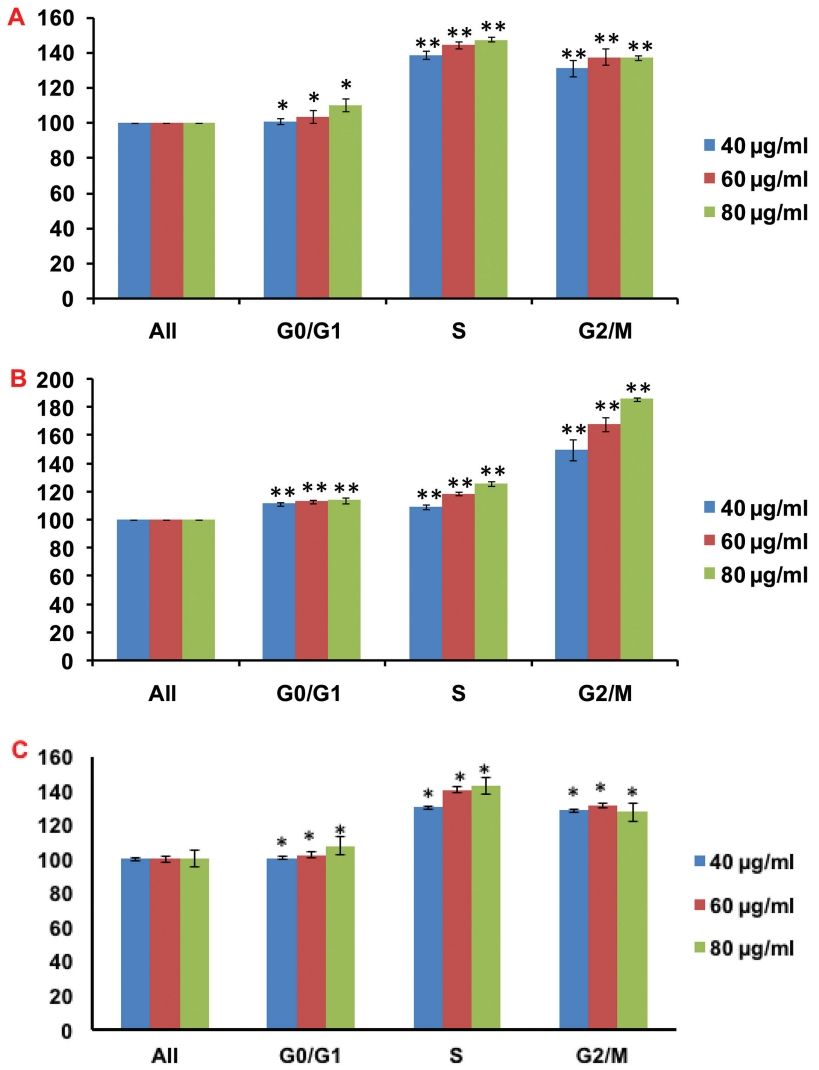


Figure 7. Cell cycle phase dependent uptake of ZnO NPs. A431 cells in different cell cycle phases were exposed to a range of ZnO NPs concentrations (40, 60 and 80 µg/ml) for (**A**) 6 h and (**B**) 24 h. (**C**) HaCaT cells exposed to a range of ZnO NPs concentrations for 6 h. Values represents mean ± SEM of three experiments for each concentrations. *$P < 0.05$ and **$P < 0.001$, when compared with control.

Table 1. ZnO NPs uptake rates in different phases of the cell cycle in A431 cells respect to control

Time	ZnO NPs (µg/ml)	Control	G_0/G_1 phase	S phase	G_2/M phase
	40	100	100.88 ± 1.82	138.87 ± 2.28	131.16 ± 4.63
6 h	60	100	103.87 ± 3.56	144.50 ± 2.04	137.71 ± 4.73
	80	100	110.22 ± 3.71	147.66 ± 1.33	137.21 ± 1.37
	40	100	111.29 ± 1.31	109.08 ± 1.80	149.74 ± 7.54
24 h	60	100	112.87 ± 0.94	118.45 ± 1.38	168.01 ± 5.18
	80	100	113.67 ± 1.93	125.53 ± 1.53	185.74 ± 1.47

Data represents mean ± SEM of three independent experiments.

which prevents the aggregation of NPs (26–29). Additionally, the protein corona plays an important role in the internalisation of NPs into the cells.

The cytotoxic potential of ZnO NPs was assessed using multiple assays, as it provides more reliable data while ignoring the interference of the dyes with NPs (30–33). A431 cells were exposed to ZnO NPs at different concentrations (1–200 µg/ml) and time points (6, 24 and 48 h). MTT and NR uptake assays were employed for cytotoxicity assessment. MTT represents mitochondrial activity and NR provides lysosomal activity of the cells. Both assays revealed a time and concentration dependent cytotoxicity of ZnO NPs, though with some variation. In MTT assay, the cytotoxicity appeared from 60 µg/ml concentration while NRU assay showed cytotoxicity from 100 µg/ml concentration. This is due to differences in the principles of both the cytotoxicity assays (30). MTT (3-(4, 5-dimethylthiazolyl-2)-2, 5-diphenyltetrazolium bromide) is a yellow tetrazolium which gets reduced by metabolically active cells by the dehydrogenase enzymes and generates reducing equivalents such as NADH

Downloaded from https://academic.oup.com/mutage/article/31/4/481/1751667 by Ahmedabad University user on 01 May 2025

and NADPH. The resulting intracellular purple formazan is solubilised and quantified by spectrophotometric means while NR is a vital dye which is incorporated into the lysosomes by active transport whereas non-viable cells do not take up the dye.

ROS plays a key role in a variety of physiological and cellular events including oxidative stress, apoptosis, protein and DNA damage (34). We observed a significantly enhanced ROS production on exposure to ZnO NPs after 6 h in A431 cells. Because the NPs have small size, they can easily enter into the cells and can induce oxidative stress by generating free radicals (35).

The internalisation of NPs was confirmed by flow cytometer and concentration-dependent increase in the SSC intensity of the treated cells. Increase in SSC intensity is an evidence of uptake of NPs (36–38). We also compared the uptake of ZnO NPs in non-cancerous cell line HaCaT (human keratinocyte cell line) and we found almost similar uptake pattern in the uptake of ZnO NPs in cancerous (A431) and non-cancerous cells (HaCaT) (Figure 7C).

To study the difference in rate of uptake of NPs in different cell cycle phases, cell cycle progression was monitored after exposure to ZnO NPs. A schematic for the same is represented in Figure 8. Cell cycle represents a series of events that allows cells to grow, proliferate and further protects the cells from DNA damage. Incubation of cells with ZnO NPs for 6, 24 and 48 h resulted in slight S and G_2/M phase arrest in A431 cells. The cell cycle arrest represents a survival mechanism that provides an opportunity to the cancerous cells to repair its own DNA damage. However, induction of cell cycle arrest is often the basis of anticancer therapeutics (39).

Earlier Kim *et al.* (20) discussed the role of cell cycle in NP uptake, and the uptake were ranked according to G_2/M > S > G_0/G_1.The other properties of NPs such as size, shape, charge and the composition of protein corona also influences the cellular uptake of NPs (40–43). Once NPs enter into a biological fluid, their surface are coated with a layer of biomolecules such as proteins and lipids which demonstrated to have a key impact on the biological behaviour of NPs including cellular uptake (44). NP–protein corona complex formation also depends on the cell cycle phases, because of the different expression of membrane proteins through the cell cycle phases which in turn affects cellular uptake (21). Therefore, in this study we assessed the cell cycle-dependent cellular uptake of ZnO NPs in A431 cells. Cell cycle synchronisation was performed for evaluating the uptake of NPs by cells in different cell cycle phases. Our results indicated that cells in different phases of cell cycle showed a difference in the uptake of ZnO NPs in the order of: G_2/M > S > G_0/G_1 after 24 h of exposure. However, in case of 6 h exposure, the cellular uptake of the NPs were ranked as S > G_2/M > G_0/G_1. At initial exposure time (6 h), cells synchronised in S and G_2/M phase showed a higher uptake, whereas the cells synchronised in G_0/G_1 phase showed lesser uptake as compared to S and G_2/M phase. Greater differences started to appear once the cells had divided as observed after 24-h exposure of NPs. The cells in G_0/G_1 phase showed a reduced NP uptake, as compared with other cells. This can be due to the difference in the incubation time of the NPs after cell division, as the cells in G_0/G_1 phase have just divided and had less time to internalise the NPs. In G_2/M phase cells have not yet divided, and therefore have accumulated NPs for longer time, whereas cells in S phase have accumulated NPs after cell division. Hence, it can be extrapolated from the observed data that in a cell population the concentration of internalised NPs varies through the cell cycle phases.

Cancerous cells are known to divide faster as compared with the normal counterparts, hence pass through the G_2/M phase more frequently. Cancerous cells also exhibit higher uptake of NPs as compared with healthy cells. Higher uptake of silicon carbide bases NPs has been reported in cancer cells (HSC-2) as compared with non-cancerous cells (3T3-L1) (45). NPs have bio-applications such as targeted therapies because they can cross biological barriers and distribute within cells by energy dependent pathway (1,39,46). Many chemotherapeutics are

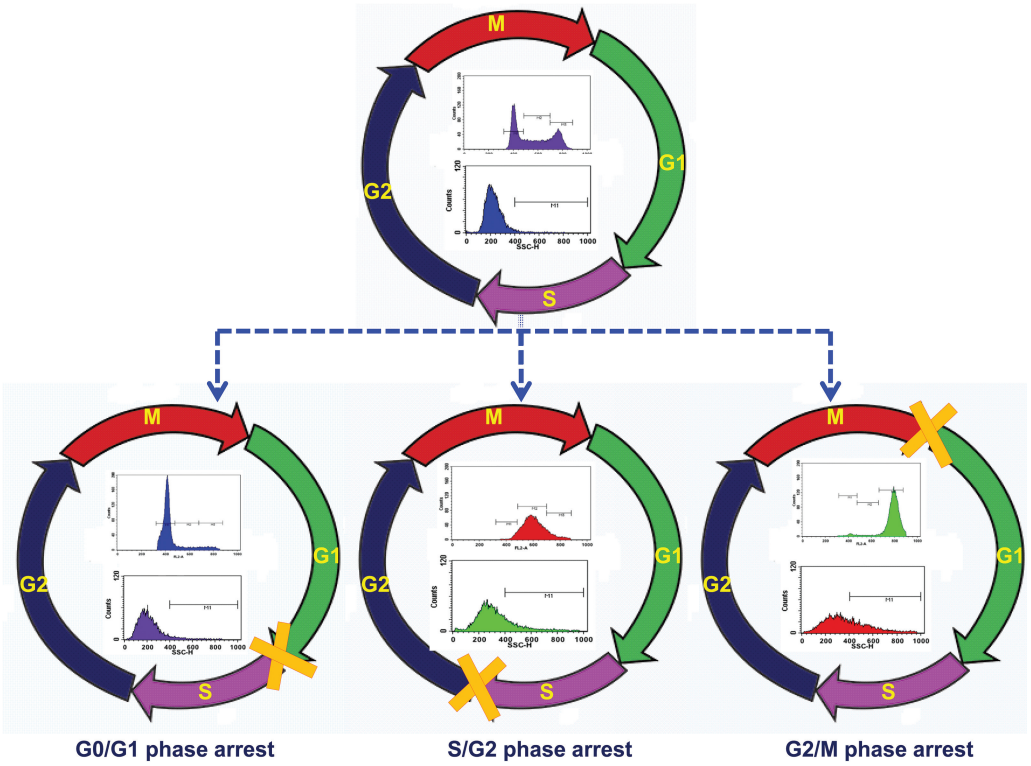


Figure 8. Schematic showing the study design.

Downloaded from https://academic.oup.com/mutage/article/31/4/481/1751667 by Ahmedabad University user on 01 May 2025

known to affect the cell cycle distribution. For example, chemotherapeutic drugs (docetaxel and paclitaxel) arrest cells in G_2/M phase and they are widely used in clinical field for the treatment of various cancers (47,48). Thus, a combined therapy, where one agent or compound (chemotherapeutic drug) arrest cells and the other deliver the therapy, can be exploited for enhanced tumour delivery of NPs.

Our results demonstrated that ZnO NPs induce cell death at high concentrations, and at lower concentrations they induce cell cycle arrest in S and G_2/M phase by intracellular ROS generation in A431 cells. For therapeutics, the extent of cellular internalisation of the NPs must be controlled. The physiological characteristics of the NPs possess a significant role in NPs uptake. The present study also demonstrated that cell cycle progression affects cellular uptake of NPs in A431 cells. Thus from the study, a combined therapy can be proposed for treating complex diseases like cancer, in which one compound arrests cell division (G_2/M phase arrest) and NPs delivers the drug or therapy.

Funding

Department of Biotechnology, Government of India under the project 'NanoToF: Toxicological evaluation and risk assessment on Nanomaterials in Food' (grant number BT/PR10414/PFN/20/961/2014); the European Union Seventh Framework Programme (FP7/2007–2013) under grant agreement No. 263147 (NanoValid – Development of reference methods for hazard identification, risk assessment and LCA of engineered nanomaterials); the Gujarat Institute for Chemical Technology – GICT (financial assistance to Centre for Nanotechnology Research and Applications – CENTRA).

Conflict of interest statement: None declared.

References

1. Oberdörster, G. (2010) Safety assessment for nanotechnology and nanomedicine: concepts of nanotoxicology. *J. Intern. Med*., 267, 89–105.
2. Mudshinge, S. R., Deore, A. B., Patil, S. and Bhalgat, C. M. (2011) Nanoparticles: emerging carriers for drug delivery. *Saudi Pharm. J*., 19, 129–141.
3. Panyam, J. and Labhasetwar, V. (2003) Biodegradable nanoparticles for drug and gene delivery to cells and tissue. *Adv. Drug Deliv. Rev*., *55*, 329–347.
4. Nie, S., Xing, Y., Kim, G. J. and Simons, J. W. (2007) Nanotechnology applications in cancer. *Annu. Rev. Biomed. Eng*., 9, 257–288.
5. Rasmussen, J. W., Martinez, E., Louka, P. and Wingett, D. G. (2010) Zinc oxide nanoparticles for selective destruction of tumor cells and potential for drug delivery applications. *Expert Opin. Drug Deliv*., 7, 1063–1077.
6. Hanley, C., Layne, J., Punnoose, A., Reddy, K. M., Coombs, I., Coombs, A., Feris, K. and Wingett, D. (2008) Preferential killing of cancer cells and activated human T cells using ZnO nanoparticles. *Nanotechnology*, 19, 295103.
7. Wang, H., Wingett, D., Engelhard, M. H., *et al*. (2009) Fluorescent dye encapsulated ZnO particles with cell-specific toxicity for potential use in biomedical applications. *J. Mater. Sci. Mater. Med*., 20, 11–22.
8. Dash, S. K., Ghosh, T., Roy, S., Chattopadhyay, S. and Das, D. (2014) Zinc sulfide nanoparticles selectively induce cytotoxic and genotoxic effects on leukemic cells: involvement of reactive oxygen species and tumor necrosis factor alpha. *J. Appl. Toxicol*., 34, 1130–1144.
9. Farokhzad, O. C. and Langer, R. (2009) Impact of nanotechnology on drug delivery. *ACS Nano*, 3, 16–20.
10. Yuan, Q., Hein, S. and Misra, R. D. (2010) New generation of chitosan-encapsulated ZnO quantum dots loaded with drug: synthesis, characterization and in vitro drug delivery response. *Acta Biomater*., 6, 2732–2739.
11. Lin, W., Xu, Y. and Huang, C. C. (2009) Toxicity of nano- and micro-sized ZnO particles in human lung epithelial cells. *J. Nanopart. Res*., 11, 25–39.
12. Sharma, V., Anderson, D. and Dhawan, A. (2012) Zinc oxide nanoparticles induce oxidative DNA damage and ROS-triggered mitochondria mediated apoptosis in human liver cells (HepG2). *Apoptosis*, 17, 852–870.
13. Akhtar, M. J., Ahamed, M., Kumar, S., Khan, M. M., Ahmad, J. and Alrokayan, S. A. (2012) Zinc oxide nanoparticles selectively induce apoptosis in human cancer cells through reactive oxygen species. *Int. J. Nanomed*., 7, 845–857.
14. Patel, P., Kansara, K., Shah, D., Vallabani, N. V., Shukla, R. K., Singh, S., Dhawan, A. and Kumar, A. (2014) Cytotoxicity assessment of ZnO nanoparticles on human epidermal cells. *Mol. Cytogenet*., 7(Suppl. 1), 81.
15. Senapati, V. A., Kumar, A., Gupta, G. S., Pandey, A. K. and Dhawan, A. (2015) ZnO nanoparticles induced inflammatory response and genotoxicity in human blood cells: A mechanistic approach. *Food Chem. Toxicol*., 85, 61–70.
16. Salvati, A., Aberg, C., dos Santos, T., Varela, J., Pinto, P., Lynch, I. and Dawson, K. A. (2011) Experimental and theoretical comparison of intracellular import of polymeric nanoparticles and small molecules: toward models of uptake kinetics. *Nanomedicine*, 7, 818–826.
17. Kim, J. A., Åberg, C., de Cárcer, G., Malumbres, M., Salvati, A. and Dawson, K. A. (2013) Low dose of amino-modified nanoparticles induces cell cycle arrest. *ACS Nano*, 7, 7483–7494.
18. Treuel, L., Jiang, X. and Nienhaus, G. U. (2013) New views on cellular uptake and trafficking of manufactured nanoparticles. *J. R. Soc. Interface*, 10, 20120939.
19. Salatin, S., Maleki Dizaj, S. and Yari Khosroushahi, A. (2015) Effect of the surface modification, size, and shape on cellular uptake of nanoparticles. *Cell Biol. Int*., 39, 881–890.
20. Kim, J. A., Åberg, C., Salvati, A. and Dawson, K. A. (2012) Role of cell cycle on the cellular uptake and dilution of nanoparticles in a cell population. *Nat. Nanotechnol*., 7, 62–68.
21. Boucrot, E. and Kirchhausen, T. (2007) Endosomal recycling controls plasma membrane area during mitosis. *Proc. Natl. Acad. Sci. U. S. A*., 104, 7939–7944.
22. Mosmann, T. (1983) Rapid colorimetric assay for cellular growth and survival: application to proliferation and cytotoxicity assays. *J. Immunol. Methods*, 65, 55–63.
23. Borenfreund, E. and Puerner, J. A. (1985) Toxicity determined in vitro by morphological alterations and neutral red absorption. *Toxicol. Lett*., 24, 119–124.
24. Wan, C. P., Myung, E. and Lau, B. H. (1993) An automated micro-fluorometric assay for monitoring oxidative burst activity of phagocytes. *J. Immunol. Methods*, 159, 131–138.
25. Shukla, R. K., Sharma, V., Pandey, A. K., Singh, S., Sultana, S. and Dhawan, A. (2011) ROS-mediated genotoxicity induced by titanium dioxide nanoparticles in human epidermal cells. *Toxicol. In Vitro*, 25, 231–241.
26. Lynch, I., Salvati, A. and Dawson, K. A. (2009) Protein-nanoparticle interactions: what does the cell see? *Nat. Nanotechnol*., 4, 546–547.
27. Dhawan, A. and Sharma, V. (2010) Toxicity assessment of nanomaterials: methods and challenges. *Anal. Bioanal. Chem*., 398, 589–605.
28. Kumar, A., Pandey, A. K., Singh, S. S., Shanker, R. and Dhawan, A. (2011) Engineered ZnO and TiO(2) nanoparticles induce oxidative stress and DNA damage leading to reduced viability of *Escherichia coli*. *Free Radic. Biol. Med*., 51, 1872–1881.
29. Elsaesser, A. and Howard, C. V. (2012) Toxicology of nanoparticles. *Adv. Drug Deliv. Rev*., 64, 129–137.
30. Sharma, V., Shukla, R. K., Saxena, N., Parmar, D., Das, M. and Dhawan, A. (2009) DNA damaging potential of zinc oxide nanoparticles in human epidermal cells. *Toxicol. Lett*., 185, 211–218.
31. Kansara, K., Patel, P., Shah, D., Shukla, R. K., Singh, S., Kumar, A. and Dhawan, A. (2015) TiO_2 nanoparticles induce DNA double strand breaks and cell cycle arrest in human alveolar cells. *Environ. Mol. Mutagen*., 56, 204–217.
32. Guadagnini, R., Halamoda Kenzaoui, B. and Walker, L. (2012) Toxicity screenings of nanomaterials: challenges due to interference with assay processes and components of classic in vitro tests. *Nanotoxicology*, 9, 13–24.
33. Kroll, A., Pillukat, M. H., Hahn, D. and Schnekenburger, J. (2012) Interference of engineered nanoparticles with in vitro toxicity assays. *Arch. Toxicol*., 86, 1123–1136.

Downloaded from https://academic.oup.com/mutage/article/31/4/481/1751667 by Ahmedabad University user on 01 May 2025

34. Luo, C., Urgard, E., Vooder, T. and Metspalu, A. (2011) The role of COX-2 and Nrf2/ARE in anti-inflammation and antioxidative stress: aging and anti-aging. *Med. Hypotheses*, 77, 174–178.
35. Borm, P. J., Robbins, D., Haubold, S., *et al.* (2006)The potential risks of nanomaterials: a review carried out for ECETOC. *Part Fibre Toxicol.* 3, 11.
36. Suzuki, H., Toyooka, T. and Ibuki, Y. (2007) Simple and easy method to evaluate uptake potential of nanoparticles in mammalian cells using a flow cytometric light scatter analysis. *Environ. Sci. Technol.*, 41, 3018–3024.
37. Kumar, A., Pandey, A. K., Singh, S. S., Shanker, R. and Dhawan, A. (2011) A flow cytometric method to assess nanoparticle uptake in bacteria. *Cytometry. A*, 79, 707–712.
38. Kumar, A. and Dhawan, A. (2013) Genotoxic and carcinogenic potential of engineered nanoparticles: an update. *Arch. Toxicol.*, 87, 1883–1900.
39. Schwartz, G. K. and Shah, M. A. (2005) Targeting the cell cycle: a new approach to cancer therapy. *J. Clin. Oncol.*, 23, 9408–9421.
40. Chithrani, B. D., Ghazani, A. A. and Chan, W. C. (2006) Determining the size and shape dependence of gold nanoparticle uptake into mammalian cells. *Nano Lett.*, 6, 662–668.
41. He, C., Hu, Y., Yin, L., Tang, C. and Yin, C. (2010) Effects of particle size and surface charge on cellular uptake and biodistribution of polymeric nanoparticles. *Biomaterials*, 31, 3657–3666.
42. Cho, E. C., Zhang, Q. and Xia, Y. (2011) The effect of sedimentation and diffusion on cellular uptake of gold nanoparticles. *Nat. Nanotechnol.*, 6, 385–391.
43. Lesniak, A., Campbell, A., Monopoli, M. P., Lynch, I., Salvati, A. and Dawson, K. A. (2010) Serum heat inactivation affects protein corona composition and nanoparticle uptake. *Biomaterials*, 31, 9511–9518.
44. Pietroiusti, A. and Campagnolo, L. (2013) Interactions of engineered nanoparticles with organs protected by internal biological barriers. *Small*, 9, 1557–1572.
45. Serdiuk, T., Lysenko, V., Mognetti, B., Skryshevsky, V. and Géloën, A. (2013) Impact of cell division on intracellular uptake and nuclear targeting with fluorescent SiC-based nanoparticles. *J. Biophotonics*, 6, 291–297.
46. Kagan, V. E., Shi, J., Feng, W., Shvedova, A. A. and Fadeel, B. (2010) Fantastic voyage and opportunities of engineered nanomaterials: what are the potential risks of occupational exposures? *J. Occup. Environ. Med.*, 52, 943–946.
47. Cheetham, P. and Petrylak, D. P. (2013) Tubulin-targeted agents including docetaxel and cabazitaxel. *Cancer J.*, 19, 59–65.
48. Gao, H., Hu, G., Zhang, Q., Zhang, S., Jiang, X. and He, Q. (2014) Pretreatment with chemotherapeutics for enhanced nanoparticles accumulation in tumor: the potential role of G_2 cycle retention effect. *Sci. Rep.*, 4, 4492.

Downloaded from https://academic.oup.com/mutage/article/31/4/481/1751667 by Ahmedabad University user on 01 May 2025